Original Article

Effect of Reconstruction Filters on Ultrasound Computed Tomography Image Quality in Two Different Detector Arrangements: a Preliminary Simulation Study

Razieh Solgi [1,2], Masoumeh Gity [3,4], Hojjat Mahani [5], Hossein Ghadiri [1,2,*]

1- Department of Medical Physics and Biomedical Engineering, Tehran University of Medical Sciences, Tehran, Iran.

2- Research Center for Molecular and Cellular Imaging, Tehran University of Medical Sciences, Tehran, Iran.

3- Advanced Diagnostic and Interventional Radiology Research Center (ADIR), Tehran University of Medical Sciences, Tehran, Iran.

4- Department of Radiology, Medical Imaging Center, Tehran University of Medical Sciences, Tehran, Iran.

5- Radiation Application Research School, Nuclear Science and Technology Research Institute, Tehran, Iran.

Received:4 March 2018
Accepted:26 may 2018

ABSTRACT

Purpose- In soft tissues, tumors have generally different sound speeds than normal tissues, so that sound speed images could be used to characterize breast cancer and to study the tumor invasion process. Ultrasound Computed Tomography (UCT) has a great potential to provide quantitative estimations of physical properties of normal and abnormal tissues that provides accurate characterization capability for breast cancer. The goal of this study is a comparison of two different detector arrangement and image reconstruction filters on image quality parameters in fan-beam back projection method to introduce the modified arrangement and filter to achieve high-quality USCT images.

Materials and methods- Two USCT systems with two different detector arrangement of the ultrasound array, ring-shape and parallel shape, have been simulated and Point Spread Function (PSF), Modulate Transform Function (MTF) and spatial resolution are three image quality parameters, have been investigated in both systems. In this study, a modified filter introduced that apply on the sinogram in two dimensions in spite of the Ram-Lak that apply on sinogram in one dimension.

Result- These study results show that the spatial resolution affected by not only detector arrangement but also reconstruction filters. In addition, applying the modified filter improves the resolution of the ring-shaped system and destroy the resolution of the line one and we have higher resolution in the modified filter than Ram-Lak.

Conclusion- The result suggests that to have high-resolution USCT images, the difference filters specially modified filter can be used and ring-shaped system has higher resolution images than line one.

Keywords:
Fan Beam back Projection;
Image Quality;
Reconstruction Filters;
Ultrasound Computed Tomography.

1. Introduction

X-ray mammography, MRI, and ultrasound are some of the common techniques used for breast cancer detection. In spite of X-ray, mammography is the standard modality clinically used for breast imaging. Mammography sensitivity decreases when imaging dense breast tissues which is prevalent among young women. Clinical studies demonstrate that ultrasound can find more and smaller cancers in dense breast

*Corresponding Author:
Hossein Ghadiri, PhD
Department of Medical Physics and Biomedical Engineering, Tehran University of Medical Sciences, Tehran, Iran.
Tel: (+98)2166439831, Fax: (+98)2166438630.
Email: h-ghadiri@tums.ac.ir

women, where mammography might miss them [1-2]. Therefore, many researchers are working on automated whole-breast ultrasound scanning systems. Ultrasound Computed Tomography (UCT) is a medical imaging modality intended as an alternative to mammography and conventional ultrasound imaging for breast cancer diagnostics. UCT can provide quantitative images of acoustical parameters such as the speed of sound that is impossible in conventional ultrasound imaging [3, 4].

There are three modes of acoustic imaging; transmission, reflection, and diffraction [5]. Transmission imaging encompasses Speed Of Sound (SOS) wave imaging and the attenuation of those waves. Transmission imaging of the breast has been actively studied for enhanced tumor detection and characterization [6-10]. Many types of reconstruction methods have been applied to the ultrasound medical imaging that diffraction tomography [11], transmission tomography [12-14] and reflection tomography [15-17] are most common. In this paper, transmission mode UCT is selected in order to reconstruct SOS map. There are a number of approaches to reconstruct images from sets of projections [18]. The iterative and back projection techniques [19, 20] are the two common methods, which back projection technique is much simpler in use and needs a shorter processing time compared to the iterative method. So this method was selected as the preferred method of reconstruction in this work. The filtered back projection technique is based on considering a straight path for ray propagation through the material. One assumption that was considered in the reconstruction was that the ultrasound wave propagated along a straight line and was received by the corresponding receiver element on the opposite side. The UCT geometry affects the image quality parameters too, so the different prototype systems have been established [21, 22] and researchers are investigating the more appropriate transducer shape array to have high-quality images.

In this study, we have investigated the two transducer shape arrays, ring, and parallel shape, and have compared the image quality parameters. At first, the models of ring-shaped and parallel-shaped systems are established, then the propagation of ultrasound wave in simulated systems and interaction between waves and object are numerically simulated by COMSOL multiphysics software (Version 5.2). After that, the set of projections is reconstructed through filter fan beam back projection by applying different reconstruction filters. Ultimately, image quality parameters were calculated and the effect of filters was investigated.

2. Material and Method

2.1. System Simulation

Two arrays of UCT system, a ring-shaped and a parallel-shaped¸ are simulated by COMSOL Multiphysics 5.2. A ring-shaped system is a ring with 20 cm diameter that is surrounded with 130 transducers. The transducers surround a phantom. It means that one transducer is a transmitter, and all the others are receivers which arelocated in a semicircle-shaped in the opposed side if transmitter. The phantom rotates 360 degrees around the system axis rotation by the rotation step of 1.41 in degree to have 256 projection (Figure. 1a). The receiver transducers are located in a line, in the parallel system (Figure. 1b). All the parameters such as transducer size, number of transducers, materials, phantom, etc. are in the same in both systems. As shown in Figure. 1, the circle phantom is immersed in water and water temperature is approximately equal to body temperature (37 ^{0}C). The phantom designed for the calculation Point Spread Function (PSF) and the Modulate Transform Function (MTF) has been shown in Figure. 1 which is a homogenous 16 cm-phantom of soft tissue with 1470 m/s speed of sound and a centered defect with a radius of 0.8 mm with the speed of sound three times bigger than the background to satisfy the Nyquist frequency. This phantom is a spacial frequency phantom.

The Active transducer operating at the 1.5 MHz frequency and the received signals are sampled at a rate of 50 MHz in both systems. The Time Of Flight (TOF) of the first arrival signal between transmitter and receivers is calculated. This value for all transmitters and receivers create the sinogram, a matrix with its columns and rows being the number of projections and detectors respectively.

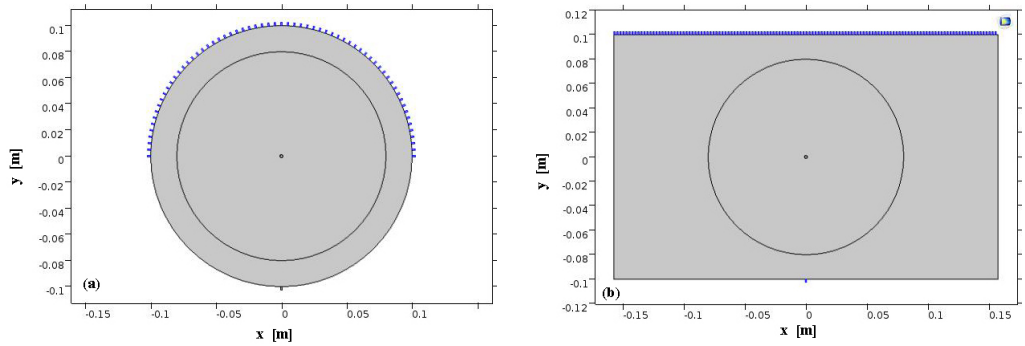

Figure 1. (a) Ring-shaped array system, (b) Parallel-shaped array system.

2.2. Fan Beam Filter Back Projection Reconstruction Method

The fan-beam back-projection method could be applied on two kinds of detectors, namely arc-shaped and line-shaped. To compare the two geometries, we have simulated fan beam back-projection method with curved and line detectors for image reconstruction. The whole steps of reconstruction is illustrated in Figure. 2 and contains the following steps: fan-beam projection generation, filtering and weighted back projection. Note that the object is denoted *O(x,y)* and the reconstructed object is *O(x',y')*.

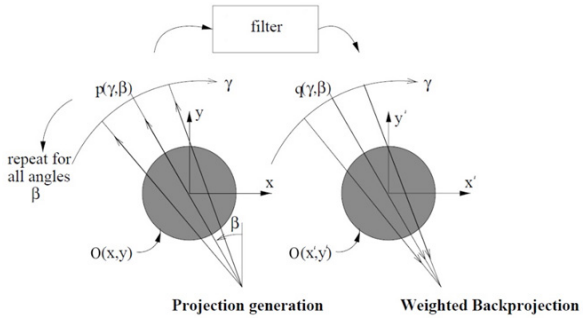

Figure 2. Fan-beam filter back-projection with curve detectors.

The fan-beam projection $p_f(\gamma,\beta)$ contains line integrals through *O(x,y)* as the geometry in Figure. 2 illustrates.

Then, a filter is applied according to:

$$q_f(\gamma,\beta) = \mathrm{F}_\gamma^{-1}\left[\mathrm{F}_\gamma\left(p_f(\gamma,\beta)\right).\mathrm{F}_\gamma\left(g(\gamma)\right)\right] \quad (1)$$

Where F_γ denotes the Fourier transform in the γ -direction, F_γ^{-1} denotes the inverse Fourier transform and $g(\gamma)$ denotes the filter and $q(\gamma,\beta)$ denotes the filtered projections.

The weighted back-projection by Equation(2) and Equation(3):

$$O(x',y') = \int_0^{2\pi} \frac{1}{L(x,y,\beta)^2} q_f(\gamma(x,y,\beta).\beta)d\beta \quad (2)$$

$$L(x,y,\beta)^2 = (R - xsin\beta + y\cos\beta)^2 + (xcos\beta + ysin\beta)^2 \quad (3)$$

Includes a space-dependent factor, $1/L^2$ where L is the distance between the actual point and the source and R is the distance between the origin and the source.

Five different filters (Ram-Lak, Shepp-Logan, Cosine, Hamming, and Hann) were applied during back projection to manipulate the reconstructed images. Each filter was defined by modifying the ideal Ramp filter (which is the Ram-Lak filter) in the frequency domain according to the window needed to emphasize high frequencies [23] as in (4) below.

$$H(\omega) = |\omega|W(\omega) \quad (4)$$

where ω is the spatial frequency and $W(\omega)$ is defined for each filter as Ram-Lak filter: *rect* (ω /2), Shepp–Logan filter: multiplies the Ram-Lak filter by a sinc function, *sinc* (ω /2), Cosine filter: multiplies the Ram-Lak filter by a Cosine function, *cos* (ω /2), Hamming filter: multiplies the Ram-Lak filter by a Hamming window, (0.54+0.46 *cos*(ω), Hann filter: multiplies Ram-Lak filter by a Hann window, (0.5+ 0.5 *cos* (ω)).

The amplitude of frequency response for each filter is depicted in Figure. 3 [24].

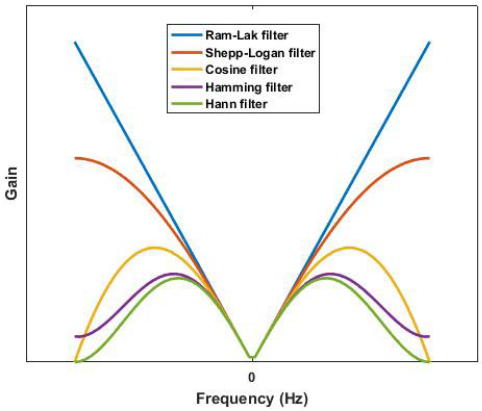

Figure 3. Frequency response curves for various reconstruction filters.

2.3. Resolution Recovery

The pulse propagates circular in the medium because of the thin piezoelectric width so that the image of the objects with more distance of transmitter become more blured and the resolution destroys in that position, because of that we can use an appropriate filter according to the positions. It means that each row and column of sinogram convolves with a different filter that the coordinate of sinogram determines the filter shape [25].

Equation (5) shows the modified filter equation.

$$Modified\ Filter = \sqrt{10X^2 + 4Y^2} \quad (5)$$

That X and Y are the x-direction and y-direction of the sinogram.

All the common reconstruction filters, such as Ram-Lak filter were applied to each row of the sinogram, in order to improve the image resolution commonly. It means each row of the sinogram is transformed to furrier space and multiplied into the filter, in this way all the rows are multipled by the same filter, while the modified filter is designed to multiple a 2D filter into the sinogram which increases the high-frequency components more than low frequencies in two dimensions. Then, the filtered sinogram is transferred to domain space and then reconstructed to the speed of sound images. The coefficient of the filter is chosen in such a way that it is a rectangle filter in the same size of the sinogram. Figure. 4 shows the 2D modified filter. In fact, this figure is in the frequency domain that the frequency changes in two dimensions instead of one dimension, something that happens in the Ram-Lak filter. In Ram-Lak filtering, the frequency just changes in y dimension and is constant in the x-direction.

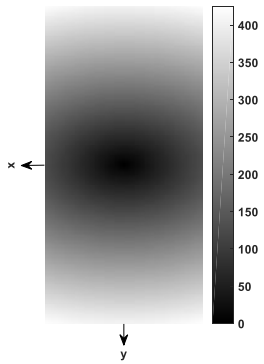

Figure 4. Two dimensional modified filter.

3. Results

To investigate the effect of the detector array arrangement and different filters on the system performance, image parameters of SOS images of filtered back projection have been calculated for both systems. To calculate the spatial resolution, full width at half maximum (FWHM) of each PSF have been calculated, Figure. 5a and Figure. 5b shows the results for systems with semicircle and line detectors respectively.

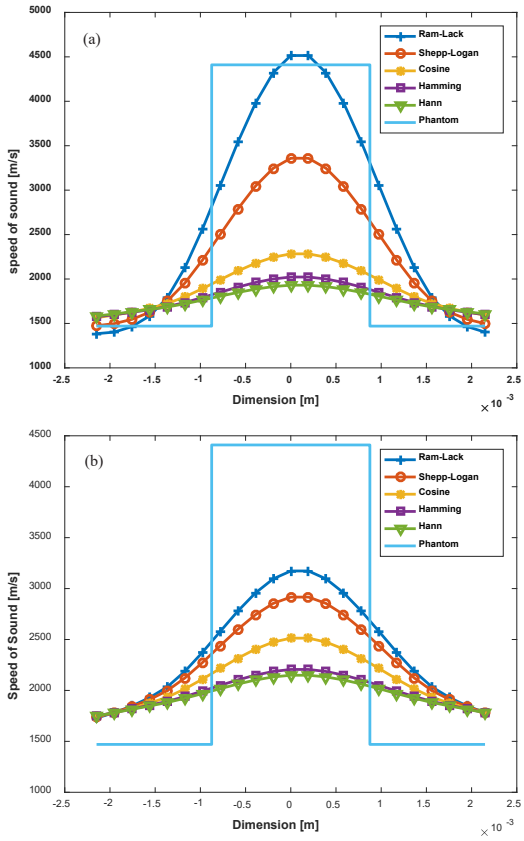

Figure 5. A comparison between the actual and reconstructed sound-speeds with different filters, across the center, for systems with (a) semicircle and (b) line detectors.

The results in Figure. 5 are summarized in Figure. 6. The result in Figure.5 and Figure. 6. shows the image resolution is more accurate in the system with a semicircle detectors array. In a semicircle detectors array, to have a more accurate resolution image is more appropriate to apply a Ram-Lak filter in back projection image reconstruction method and in line detectors, Shepp-Logan filter provides a more accurate resolution image. In two systems, filtered images with Ram-Lak provide the more accurate speed of sound images too (Figure. 5). Also applying the modified filter on the semicircle system, the FWHM of the central object is almost equal to the object size, but applying the modified filter destroyed the resolution in a system with line detectors.

MTF is calculated and the effect of different filters has been investigated for both systems. Figure. 7a and Figure. 7b show the MTF for semicircle and line detectors respectively. Figure. 7 shows the systems with semicircle detectors can show more details compared with the other.

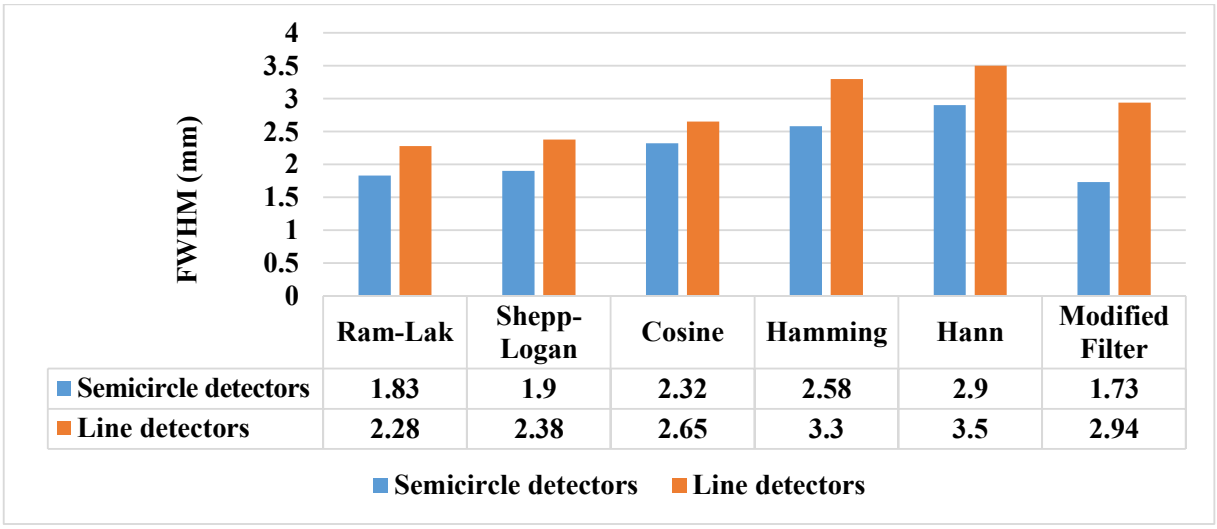

	Ram-Lak	Shepp-Logan	Cosine	Hamming	Hann	Modified Filter
Semicircle detectors	1.83	1.9	2.32	2.58	2.9	1.73
Line detectors	2.28	2.38	2.65	3.3	3.5	2.94

Figure 6. A summary of the influence of filters on resolution in both systems.

In semicircle detectors at 85 % MTF and in line detectors, at 70 % MTF, the spatial frequency is minimally varied (~1 cycle/mm for semicircle and ~1.5 cycles/mm for line). However, at 20 % MTF, the variation in spatial frequency is quite high. In semicircle detectors, a maximum spatial frequency was given by the Ram-Lak filter (~4.5 cycles/mm) and minimum (~3.5 cycles/mm) by the Hann. In line detectors, at 20 % MTF, the maximum spatial frequency is ~4 cycles/mm by using the Ram-Lak and minimum is ~3.5 cycles/mm by using the Hann filter. In comparison, in semicircle detectors, spatial resolution at 20 % MTF given by the Ram-Lak filter was 26 % higher than that given by the Hann filter whereas for line detectors there is an increase of 8.25 %. This indicates that the reconstruction filter affects the spatial resolution and hence the spatial resolution can be improved by using a filter that emphasizes high-frequency components.

4. Discussion

The main objective of our study was the comparison between two detector arrangements in UCT and the investigation of the effects of different image filters on MTF in both. In this work, we applied five common reconstruction filters, Ram-Lak, Shepp-Logan, Cosine, Hamming and Hann and a modified filter on the UCT image to investigate the effect of these on the resolution, PSF and MTF in fan beam filter back projection reconstruction method for two different ultrasonic arrays, a ring-shaped and a parallel-shaped. As mentioned in [20] for semicircle detector array, comparing all five common filters shows the Ram-Lak and Shepp-Logan filters seem to be the most optimal for improving the resolution. Also the Ram-Lak gives the highest spatial frequency and Hann gives the lowest. In comparison, in semicircle detectors, spatial resolution at 20 % MTF given by the Ram-Lak filter was 26 % higher

than that given by the Hann filter whereas for line detectors there is an increase of 8.25 %. This indicates that the reconstruction filter affects the spatial resolution and hence the spatial resolution can be improved by using a filter that emphasizes high-frequency components. As the result shows, MTF for semicircle detectors is higher than that of line detector array. Thus, the arrangement of the ultrasonic detector array has a significant effect on the image quality. As the figures show, the PSF becomes wider as the descent of the filter decreases in both arrangements, but in a system with line detectors, the PSF becomes wider and MTF is affected by this variation. As the pulse goes away in depth becomes wider and in the linear array system, the pulse puts more distance in comparison with a circular array that affects the pulse width. The more width the pulse, the more incorrect calculation of the TOF which causes the sound speed calculation. In addition, we applied a modified filter that in spite of it improving the resolution of the semicircle system, destroyed the resolution of the line system; it is because of the filter shape which is more adaptable with the system geometry in a semicircle system. According to the aforementioned reasons, the sound speed calculation of ring array detectors is more accurate than a linear one.

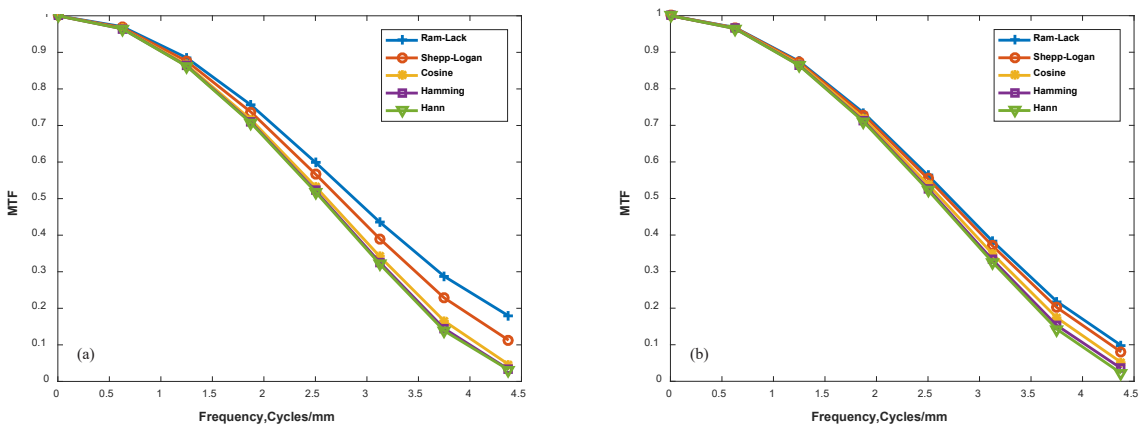

Figure7. The effect of different filters on MTF in (a) semicircle and (b) line detectors.

5. Conclusion

UCT can be used to quantitatively measure acoustic properties of the scanned region. In this paper, we compared two different detector arrays, semicircle, and line, on image quality parameters. The comparison result is important to choose the best arrangement to have high-quality images. Improving the image quality parameters of UCT images by applying optimum image processing methods help to decrease the number of transducers that cause the system cost or decrease the number of projections that help to have a faster imaging system. In comparing two arrays, we showed that the calculated sound speed was more accurate in ring-shaped than the linear one actually by applying the Ram-Lack filter, and MTF for semicircle detectors was higher than that of line detector array. We also showed that applying the modified filter improves the resolution of the semicircle system and destroyed the resolution of the line one. The modified filter act on the sinogram in two dimensions in spite of the Ram_Lak apply on sinogram in one dimension, so we had a higher resolution in the modified filter than Ram-Lak.

References

1- P. B. Gordon and, S. L. Goldenberg, “Malignant breast masses detected only by ultrasound. A retrospective review,” Cancer, vol. 76, pp. 626–630, 1995.

2- X. Ying, Y. Lin, X. Xia, B. Hu, Z. Zhu, and, P. He, “A comparison of mammography and ultrasound in women with breast disease: A receiver operating characteristic analysis,” The Breast Journal, vol. 18, pp. 130–138, 2012.

3- J. Mamou, and M. L. Oelze (Eds.), “Quantitative ultrasound in soft tissues,” Heidelberg: Springer, pp. 226, 2013.

4- JR. Jago, TA. Whittingham, “Experimental studies in transmission ultrasound computed tomography,” in Physics in medicine and biology, vol. 36, no. 11, pp. 1515, 1991.

5- L. Medina, N. González-Salido, J. Camacho, M. Pérez-Liva, JL. Herraiz, and JM. Udías, "Refraction correction in Full Angle Spatial image Compounding," in Medical Engineering Physics Exchanges/Pan American Health Care Exchanges, pp. 1-4, 2016.

6- P. J. Littrup, N. Duric, S. Azevedo, D. Chambers, J. V. Candy, S. Johnson, G. Auner, J. Rather, E. T. Holsapple, "Computerized Ultrasound Risk Evaluation (CURE) System: Development of Combined Transmission and Reflection Ultrasound with New Reconstruction Algorithms for Breast Imaging Acoustical Imaging," Acoustical Imaging, vol. 26, pp. 175-182, 2002.

7- N. Duric, P. J. Littrup, E. Holsapple, A. Babkin, R. Duncan, A. Kalinin, R. Pevzner, and M. Tokarev, "Ultrasound tomography of breast tissue," in Medical Imaging, vol. 5035, pp. 24, May 2003.

8- P. L. Carson, C. R. Meyer, A. L. Scherzinger, and T. V. Oughton, "Breast imaging in coronal planes with simultaneous pulse echo and transmission ultrasound," Science, vol. 214, pp. 1141-1143, December 1981.

9- H. Gemmeke and N. Ruiter, "3D ultrasound computer tomography for medical imaging," Nuclear Instruments and Methods in Physics, vol. 580, pp. 1057-1065, October 2007.

10- J. S. Schreiman, J. J. Gisvold, J. F. Greenleaf, and R. C. Bahn, "Ultrasound transmission computed tomography of the breast," Radiology, vol. 150, pp. 523-530, February 1984.

11- D. Hemzal, I. Peterlik, J. Rolecek, J. Jan, N. Ruiter, and R. Jirik, "3D simulation of diffraction in ultrasonic computed tomography," The 30th Annual International Conference of the IEEE Engineering in Medicine and Biology Society, pp. 454-457, 2008.

12- K. Xiong, Y. Zhang, Z. Zhang, S. Wang, Z. Zhong, "PA-NEMO: Proxy mobile IPv6-aided network mobility management scheme for 6LoWPAN Elektronika in Elektrotechnika," vol. 20, pp. 98-103, 2014.

13- Y. Qi, M. Tang, and M. Zhang, "Mass customization in flat organization: The mediating role of supply chain planning and corporation coordination," in Journal of Applied Research and Technology, vol. 12, pp. 171-181, 2014.

14- J.W. Jeong, D.C. Shin, S.H. Do, C. Blanco, N.E. Klipfel, D.R. Holmes, L.J. Hovanessian-Larsen, and V.Z. Marmarelis, "Differentiation of cancerous lesions in excised human breast specimens using multiband attenuation profiles from ultrasonic transmission tomography," Journal of Ultrasound in Medicine, vol. 27, pp. 435-451, 2008.

15- J. Nebeker, and T.R. Nelson, "Imaging of sound speed using reflection ultrasound tomography," Journal of Ultrasound in Medicine, vol. 31, pp. 1389-1404, 2012.

16- M. Birk, M. Zapf, M. Balzer, N. Ruiter, and, J. Becker, "A comprehensive comparison of GPU-and FPGA-based acceleration of reflection image reconstruction for 3D ultrasound computed tomography," Journal of Real-time Image Processing vol. 9, pp. 159-170, 2014.

17- C. Zhang, L. Huang, and Z. Zhao, "Research on combination forecast of port cargo throughput based on time series and causality analysis," in Journal of Industrial Engineering and Management, vol. 6, pp. 124-134, 2013.

18- M. Pérez-Liva, JL. Herraiz, JM. Udías, E. Miller, BT. Cox, and BE.Treeby, "Time domain reconstruction of sound speed and attenuation in ultrasound computed tomography using full wave inversion a," in The Journal of the Acoustical Society of America, vol. 141, pp.1595-604, 2017.

19- J.T. Bushberg, "The essential physics of medical imaging," William & Wilkins, 1994.

20- M. Faramarzi, S. Ibrahim, MA. Yunus, J. Pusppanathan, "Image reconstruction methods for ultrasonic transmission mode tomography in bubbly flow regime," in Jurnal Teknologi, vol. 70, no. 3, 2014.

21- N. Duric, P. Littrup, L. Poulo, A. Babkin, R. Pevzner, E. Holsapple, O. Rama, and C. Glide, "Detection of breast cancer with ultrasound tomography: First results with the Computed Ultrasound Risk Evaluation (CURE) prototype," Med. Phys. Vol. 34, pp. 773–785, Feb. 2007.

22- L. Huang, J. Shin, T. Chen, Y. Lin, M. Intrator, K. Hanson, K. Epstein, D. Sandoval, and M. Williamson, "Breast ultrasound tomography with two parallel transducer arrays: Preliminary clinical results," in [Ultrasonic Imaging and Tomography], Bosch, J. G. and Duric, N., eds., Proc. SPIE 9419, 941916–1–10, SPIE, Bellingham, Washington, 2015.

23- K. Srinivasan, M. Mohammadi, and, J. Shepherd, "Investigation of effect of reconstruction filters on cone-beam computed tomography image quality," Australasian Physical & Engineering Sciences in Medicine, vol. 37, pp. 607-614, 2014.

24- S.W. Lee, C.L. Lee, H.M. Cho, H.S. Park, D.H. Kim, Y.N. Choi, and H.J. Kim, "Effects of reconstruction parameters on image noise and spatial resolution in cone-beam computed tomography," J. Korean Phys Soc, vol. 59, pp. 2825–2832, 2011.

25- E. O'Mahoney, I. Murray, "Evaluation of a matched filter resolution recovery reconstruction algorithm for SPECT-CT imaging," Nuclear medicine communications, vol. 1, No. 34, pp. 240-8, 2013.